[CANCER RESEARCH 63, 5291–5298, September 1, 2003]

Expression of Mammalian Paralogues of *HRAD9* and *Mrad9* Checkpoint Control Genes in Normal and Cancerous Testicular Tissue[1]

Kevin M. Hopkins, Xiaojian Wang, Ana Berlin, Haiying Hang, Harshwardhan M. Thaker, and Howard B. Lieberman[2]

Center for Radiological Research [K. M. H., X. W., H. H., H. B. L.] and Department of Pathology [A. B., H. M. T.], Columbia University College of Physicians and Surgeons, New York, New York 10032

ABSTRACT

Human and mouse paralogues of the evolutionarily conserved mammalian *HRAD9* and *Mrad9* cell cycle checkpoint control genes have been isolated and called *HRAD9B* and *Mrad9B*, respectively. *HRAD9B* encodes a protein that is 414 amino acids long and is 55% similar and 35% identical to the *HRAD9* gene product. The Mrad9B protein is 398 amino acids long and is 50% similar and 35% identical to its paralogue. We demonstrate that the encoded human protein is nuclear and can physically interact with checkpoint proteins HRAD1, HRAD9, HHUS1, and HHUS1B, much like HRAD9. Northern blot analysis to detect tissue specificity indicates that the human and mouse genes are expressed predominantly in the testis. The abundance of *HRAD9B* RNA, as judged by quantitative reverse transcription-PCR, is very low in most testicular tumors, particularly those of germ cell origin, *i.e.*, seminomas, relative to normal testis control, nonseminomas, or Leydig tumor cells. RNA levels corresponding to *HRAD17*, another checkpoint control gene, demonstrated a similar pattern, but in general, higher quantities of this message were detected in samples. Furthermore, normal/tumor tissue differences were not as dramatic or consistent from sample to sample, especially for the seminomas. Our results demonstrate for the first time that *HRAD9* and *Mrad9* are part of a gene family and reveal a new genetic element encoding a product that interacts with multiple, known cell cycle checkpoint control proteins. The findings also indicate that *HRAD9B* can serve as a biomarker in particular for testicular seminomas and might be causally related to the disease.

INTRODUCTION

Human *HRAD9* was originally identified as a structural homologue of yeast *Schizosaccharomyces pombe rad9* and is capable of at least partially complementing the radiosensitivity, hydroxyurea sensitivity, and associated checkpoint defects of a *rad9*-null mutant of this fission yeast (1). A mouse orthologue, called *Mrad9*, was also identified (2). HRAD9 is a nuclear protein (3, 4) that can be phosphorylated by ATM in response to DNA damage, an event important for G_1-S checkpoint control (5). Furthermore, there is some evidence indicating that the protein demonstrates 3′ to 5′ exonuclease activity (6). HRAD9 also functions as a cell death mediator. Recent studies revealed that the human and yeast genes are members of the BH3-domain only, proapoptotic family of Bcl-2 proteins (7, 8). Phosphorylation by c-abl (9) and protein kinase Cδ (10) is important for this activity. Human HRAD9 can bind the antiapoptotic proteins Bcl-2 and Bcl-X_L with its NH_2-terminal region and the checkpoint control-related proteins HUS1 and RAD1 with its COOH-terminal region, suggesting that the protein possesses at least two functional domains, each involved in distinct cellular responses to DNA damage (11). In terms of cell cycle checkpoint control, several groups have suggested that HRAD9-HHUS1-HRAD1 form a proliferating cell nuclear antigen-like heterotrimer clamp, sometimes referred to as the 9-1-1 complex (4), that is recruited onto damaged DNA via a clamp loader function of HRAD17. This in turn might recruit other proteins to DNA, perhaps serving as a signal to the cell cycle machinery or to facilitate repair. However, the precise molecular mechanisms involved in HRAD9-mediated signal transduction and the relationship to the proapoptotic activity of the protein remain unknown.

Recently, paralogues of human and mouse *HUS1*, deemed *HHUS1B* and *Mhus1B*, respectively, have been identified (12), and the former has been characterized in some detail. The encoded protein is structurally related to the *HHUS1*gene product and can coimmunoprecipitate with tagged HRAD9, HRAD1, and HHUS1. Furthermore, overexpression of *HHUS1B* in human 293 cells causes significant loss of clonogenicity, whereas similar studies with *HHUS1* reveal no such effect. These findings suggested that *HHUS1* and *HHUS1B* have related but not identical functions in cell cycle checkpoint control and perhaps other as of yet undefined cellular processes.

Several checkpoint control-related genes are highly expressed in testis (2, 12–20). Furthermore, loss of some, including mouse *atm*, *Brca2*, or *Mlh1*, can cause abnormal germ cell development and sterility (21–25). Checkpoint genes are also often involved in maintaining genomic integrity, and their aberrant expression can lead to cancer (26).

The majority of testicular tumors originate from germ cells (27, 28), developing first from a carcinoma *in situ* (29–31), and include two main types, seminomas and nonseminomas. Seminomas are further divided into typical or spermatocytic types, with an average age of onset of approximately 50 and 65 years, respectively. In contrast, nonseminomas are observed in men in their 20s. These are categorized as embryonal carcinoma, yolk sac carcinoma, choriocarcinoma, and teratoma, although most nonseminomas are usually a mix of different types. Testicular tumors do not always arise from germ cells but could originate from connective tissues and androgen-producing tissues or stroma. These stromal tumors are categorized as either Leydig or Sertoli tumors, depending on the cells from which they arise, and are relatively rare compared with testicular tumors of germ cell origin. Changes in specific regions of chromosomes, including those of chromosomes 1, 3, 11, and 12, have been associated with germ cell or other types of testicular cancers (27, 28, 32, 33). Furthermore, changes in levels of glycogen, germ cell/placental alkaline phosphatase, glial cell line-derived neurotrophic factor, and testis-specific protein or of the RNA corresponding to *c-Kit*, *piwi* or zinc finger genes have been associated with different types of testicular cancers (34–38). However, despite these findings, the mechanistic, genetic basis for the disease has not been established. It is clear, though, that many of the genes involved in the etiology of testicular cancers are also involved in normal spermatogenesis, and an understanding of their functions should aid in the design of more effective therapies (39).

In this report, we describe the isolation of human and mouse paralogues of *HRAD9*/*Mrad9*, called *HRAD9B* and *Mrad9B*, respectively. All four genes encode proteins that are structurally related throughout their entire lengths and thus indicate the existence of a

Received 3/17/03; revised 5/27/03; accepted 6/9/03.

The costs of publication of this article were defrayed in part by the payment of page charges. This article must therefore be hereby marked *advertisement* in accordance with 18 U.S.C. Section 1734 solely to indicate this fact.

[1] Supported by NIH Grants GM52493 and CA89816 (to H. B. L.).

[2] To whom requests for reprints should be addressed, at Center for Radiological Research, Columbia University College of Physicians and Surgeons, 630 West 168th Street, New York, NY 10032. Phone: (212) 305-9241; Fax: (212) 305-9241; E-mail: lieberman@cancercenter.columbia.edu.

Table 1 *Normal and cancerous testicular tissue samples used in this study*

Sample	Type
364N	Normal testis
364T	Seminoma
430N	Normal testis
430T	Seminoma
778N	Normal testis
778T	Seminoma
1637N	Normal testis
1637T	Nonseminomatous germ cell tumor
1203N	Normal testis
1203T	Nonseminomatous germ cell tumor
A415N	Normal testis
A415T	Nonseminomatous germ cell tumor
1364T	Seminoma
B584T	Leydig cell tumor
276	Nonseminomatous germ cell tumor
363	Nonseminomatous germ cell tumor
368A	Nonseminomatous germ cell tumor
368B	Nonseminomatous germ cell tumor
501	Nonseminomatous germ cell tumor
582	Seminoma
1493	Seminoma
1738	Nonseminomatous germ cell tumor
POCO2-5 TST	Normal fetal testis
POCO2-9 TST	Normal fetal testis
POCO2-19 TST	Normal fetal testis

gene family. Furthermore, we demonstrate that, like HRAD9 protein, the *HRAD9B* gene product can coimmunoprecipitate with the checkpoint control proteins HRAD1, HRAD9, HHUS1, and HHUS1B. However, *HRAD9B* and *Mrad9B* are expressed predominantly in testis, whereas their paralogues are expressed more universally in many different tissues. And most notably, we demonstrate that *HRAD9B* RNA abundance is markedly reduced in testicular seminomas, relative to normal tissue controls or even other types of testicular tumors, where expression is also reduced. These results suggest that *HRAD9B* could at a minimum serve as a marker for testicular tumors, and its expression may be causally related to the disease. Our findings are presented in light of current models of cell cycle checkpoint control and the genetics of testicular cancer.

MATERIALS AND METHODS

Tissue Samples. Table 1 lists and describes the normal and cancerous testicular tissue samples used in this study. Samples of frozen tissue were obtained from the Columbia Comprehensive Cancer Center Tumor Bank Facility. For each sample, 30 five-μm sections were obtained; the middle 28 portions were processed for RNA isolation and RT-PCR,[3] and the bottom and top pieces were stained with H&E (Hematoxylin and Eosin) for histological analyses.

Plasmids and DNA. PCR was used to clone *HRAD9B* and *Mrad9B*. Human and mouse testis Marathon-Ready cDNA kits (BD Biosciences Clontech, Palo Alto, CA) were used as template, along with primers (*HRAD9B*, 5′-CATGCTGAAGTGCGTGATGA-3′; *Mrad9B*, 5′-CATGCTGAAGTGCGGGATGA-3′) made by Invitrogen (Carlsbad, CA) and based on translated expressed sequence tags that have homology to the HRAD9 (accession number AAB39928) and Mrad9 (accession number AAC77365) protein sequences. These primers, in combination with the adaptor primer supplied with the Marathon cDNA kits, were used to amplify the cDNAs. PCR conditions were 1 cycle of 95°C for 5 min, then 95°C for 30 s, 57°C for 30 s, 72°C for 2 min, repeated 35 times. PCR products were TA cloned into pGEM-T (Promega, Madison, WI), and the DNA sequence of the inserts was determined to confirm that the desired product was isolated. To create an NH_2-terminal HA epitope-tagged HRAD9B, a PCR-derived product containing the *HRAD9B* ORF from pGEMT-HRAD9B was amplified using primers (5′-GAACTTCTCGAGATGCTGAAGTGCGTGATGAG-3′ and 5′-GATATCCTCGAGCCAGCTCAGCCATCATTAAG-3′), cut with *Xho*I and cloned into the *Xho*I site of pB42AD. The *HRAD9B* fragment from pB42AD was inserted into the *Xho*I site of pLexA to make pLexA-HRAD9B. pCMV-HA (BD Biosciences) was used to construct a vector able to express in human 293 cells. pCMV-HA contains an NH_2-terminal HA epitope. pCMV-HA-HRAD9B was generated by removing the *HRAD9B* fragment from pLexA-HRAD9B (made previously) using *Sal*I and ligation into the *Xho*I site of pCMV-HA. pFLAG-CMV-2-HRAD1, pFLAG-CMV-2-HRAD9, pFLAG-CMV-2-HHUS1, pFLAG-CMV-2-HHUS1B, and pHRAD9-1 containing the *HRAD9* cDNA have been described elsewhere (1, 11, 12).

Northern Analysis, RNA Isolation, and Quantitative RT-PCR. Human and mouse Multiple Tissue Northern Blots were purchased from BD Biosciences Clontech and Stratagene (La Jolla, CA). The Strip-EZ labeling kit from Ambion (Austin, TX) was used to ^{32}P label RNA antisense probes synthesized from both human and mouse *RAD9B* cDNA ORFs. *HRAD9* cDNA ORF (1) was ^{32}P labeled as well for probing Northern blots. The blots were stripped and then probed with ^{32}P-labeled β-actin cDNA.

RNA was isolated from tissue sections using the RNeasy mini-kit (Qiagen, Valencia, CA). One μg of the RNA was reverse transcribed into DNA using the Superscript reverse transcription kit (Invitrogen). The DNA was then used to PCR amplify *HRAD9B* (primers, 5′-CAACCAAGATTGCTTGCTGA-3′ and 5′-GCCAACAAACATCTCACTGTGT-3′), *HRAD9* (primers, 5′-CTCTTCTTCCAGCAATACCA-3′ and 5′-TGCTGACTCTGCAAAGCTCA-3′), *HRAD17* (primers, 5′-GATGAGGACGAAATGAATCA-3′ and 5′-CCCGATAAAACTGGTTAGGT-3′), and *GADPH* (primers, 5′-AAGGTGAAGGTCGGAGTCAA-3′ and 5′-GATGGCATGGACTGTGGTCA-3′), using the LightCycler Fast Start DNA Master SYBR Green kit (Roche, Indianapolis, IN). PCR was carried out in the LightCycler System (Roche). Cycling conditions were 1 cycle of 95°C for 10 min and 60 cycles of 95°C for 10 s, 57°C for 5 s, and 72°C for 15 s.

Coimmunoprecipitation and Western Blotting. Human 293 cells, between 50% to 80% confluent in 100-mm cell culture dishes, were transiently transfected with 2 μg of pFLAG-CMV-2 construct plasmids and 4 μg of pCMV-HA plasmids using Lipofectin Plus Reagent following protocols suggested by the manufacturer (Invitrogen). After a 48-h incubation in a 37°C, 5% CO_2 incubator, cells were lysed in 1 ml of ice-cold mammalian cell lysis buffer [150 mM NaCl, 50 mM Tris-HCl (pH 8.0), 1.5 mM $MgCl_2$, 1.5 mM $CaCl_2$, and 1% NP40]. Protein inhibitor mixture (Roche) was added. Lysate was centrifuged at 10,000 rpm for 10 min at 4°C. The supernatants were collected and precleared with 25 μl of protein A and 1 μg of normal rat serum for 1 h. The precleared supernatants were immunoprecipitated with 30 μl of anti-FLAG M2-agarose affinity gel (Sigma) overnight while continuously mixing in 1.5-ml microcentrifuge tubes on a spinning wheel at 4°C. After beads were washed with mammalian cell lysis buffer five times, 30 μl of Laemmli sample buffer (Bio-Rad, Hercules, CA) were added to each tube, and the beads were boiled for 5 min. Fifteen μl of each supernatant were run through a 10% SDS-PAGE gel and immunoblotted with anti-HA-peroxidase high-affinity antibody (Roche). Signals were visualized by chemiluminescence using enhanced chemiluminescence detection reagents (ECL; Amersham Biosciences, Piscataway, NJ) and exposing X-ray film. Similar but somewhat modified procedures were used to perform the coimmunoprecipitations in the reverse directions. Two μg of pCMV-HA constructs and 4 μg of pFLAG-CMV-2 plasmids with or without inserts were used for transient transfection. Cell lysates were precleared with protein A and 1 μg of normal mouse serum and immunoprecipitated with anti-HA affinity matrix (Roche). The primary antibody used for Western blotting was anti-FLAG M2 monoclonal antibody (Sigma), and the secondary antibody was antimouse IgG-horseradish peroxidase (Santa Cruz Biotechnology, Santa Cruz, CA). For transfection with only one plasmid, 30,000 cells were lysed in 30 μl of sample buffer. Three μl were loaded onto SDS-PAGE gels, and immunoblotting and related procedures were followed as described.

Subcellular Localization. HeLa cells (1.3×10^7) were resuspended in 300 μl of DMEM without FCS and mixed with 7.5 μg of pFLAG-CMV-2-HRAD9B or pFLAG-CMV-2-HRAD9 for 5 min at room temperature in an electroporation cuvette. Electroporation conditions described in GenePulser Electroprotocol (Survey Number 094; Bio-Rad) were followed. The GenePulserII electroporation system was used. Ten min after electroporation, cells were seeded onto coverslips and incubated overnight at 37°C in 5% CO_2. Cells were then washed with PBS (with Ca^{2+} and Mg^{2+}) and fixed with acetone/

[3] The abbreviations used are: RT-PCR, reverse transcription-PCR; HA, hemagglutinin; ORF, open reading frame; PBST, PBS and 0.5% Tween 20; DAPI, 4′,6-diamidino-2-phenylindole.

methanol (1:1) for 5 min. After washing twice in PBS, cells were permeabilized with PBS and 0.5% Triton X-100 for 10 min, rinsed twice (5 min each) in PBS, and then rinsed in PBST. Five percent milk and PBST were used to block cells at 37°C for 30 min. Cells were then incubated with 10 μg/ml anti-FLAG M2 FITC-conjugated monoclonal antibody (Sigma) diluted 1:110 in blocking milk solution at 37°C for 1 h. After three washes in PBST for 5 min each, cells were rinsed in 70% ethanol for 3 min and then rinsed in 95% ethanol for 3 min. All of the rinsing steps were performed at room temperature. Cell nuclei were stained with DAPI (Vector Laboratories, Burlingame, CA) for 5 min at room temperature. Coverslips were mounted on glass slides, and the fluorescent signal was visualized by using a Axioplan 2 imaging microscope and camera (Carl Zeiss Optical, Inc., Karlsruhe, Germany). Pictures were pseudocolored and saved using Isis software (Meta System, Altlussheim, Germany).

RESULTS

Identification and Molecular Cloning of Paralogs of *HRAD9* and *Mrad9*. A BLAST search of GenBank, using HRAD9 and Mrad9 amino acid sequences as queries, revealed the existence of highly related human and mouse cDNAs from testis (accession number 15447209) or liver (accession number 11149214) libraries, respectively. Based on the available cDNA sequences and related genomic sequences (accession number NT_009770 for HRAD9B), we used primers 5′-CATGCTGAAGTGCGTGATGA-3′ (for human) or 5′-CATGCTGAAGTGCGGGATGA-3′ (for mouse) via 3′-RACE to amplify full-length cDNAs from human or mouse testis RNA and then subsequently subcloned them into a TA vector (pGEM-T; Promega). The sequence of the genes was determined and compared with GenBank submissions to confirm that the genes were devoid of bp errors. We call these genes *HRAD9B* and *Mrad9B*, respectively. The human gene has been assigned GenBank accession number AY297459, and the mouse gene received GenBank accession number AY297460. The 5′-untranslated end of *HRAD9B* in GenBank is 23 bp. That is gleaned from the expressed sequence tag with accession number 15447209. The 3′-untranslated ends of four clones isolated from a human testis cDNA library (Clontech) range from 508 to 525 bp in length. The 5′-untranslated region of *Mrad9B* in GenBank is 34 bp (accession number 11149214). The 3′-untranslated end of four clones isolated from a mouse testis cDNA library (Clontech) can be grouped into two pairs. One pair has a stop codon similar in location to *HRAD9B*. The 3′ ends of these two clones are 239 and 361 bp, respectively. The other two cDNAs are alternatively spliced and differ from the first pair of cDNAs at 2 of the last 3 amino acids of the coding sequence and are predicted to code for 19 additional amino acids. The 3′-untranslated ends of these two clones are 277 and 304 bp. Fig. 1 illustrates a comparison of HRAD9 and HRAD9B proteins, as well as Mrad9 and its shorter paralogue. As indicated, homology extends throughout the length of the proteins and is not confined to a limited number of regions, although it is highest near the NH_2-terminal vicinity of the proteins. *HRAD9* and *HRAD9B* encoded proteins are 55% similar and 35% identical. *Mrad9* and *Mrad9B* gene products are 50% similar and 35% identical. Seventy-six percent of similarly located amino acids in HRAD9B and Mrad9B have related physiochemical properties, and 63% are identical. When the HRAD9 or Mrad9 gene products are used as query sequences in a BLAST search, the paralogues and orthologues from many different organisms are detected. Moreover, when the *HRAD9B* or *Mrad9B* encoded amino acid sequences are used to search GenBank, only HRAD9 and Mrad9 proteins, as well as numerous orthologues, are found. These include genes from *Danio rerio*, *Rattus norvegicus*, *Xenopus laevis*, *Drosophila melanogaster*, *Schizosaccharomyces pombe*, *Schizosaccharomyces octosporus*, *Arabidopsis thaliana*, and *Caenorhabditis elegans*. No paralogues other than HRAD9B and Mrad9B are detected.

To determine the intron-exon structure of the genes, the genomic versions in GenBank were compared with the ORFs of the cDNAs

```
HRAD9: 1   MKCLVTGGNVKVLGKAVHSLSRIGDELYLEPLEDGLSLRTVNSSRSAYACFLFAPLFFQQ 60
           +KC+++G  VKV GKAV +LSRI DE +L+P + GL+LR VNSSRSAY C LF+P+FFQ
HRAD9B:1   MLKCVMSGSQVKVFGKAVQALSRISDEFWLDPSKKGLALRCVNSSRSAYGCVLFSPVFFQH 61

HRAD9: 61  YQ----AATPGQDL-----LRCKILMKSFLSVFRSLAMLEKTVEKCCISLNGRSSRLVVQ 111
           YQ         +L      L+CK+ MKS L +FR L  LE+ +EKC I        ++V+Q
HRAD9B:62  YQWSALVKMSENELDTTLHLKCKLGMKSILPIFRCLNSLERNISKCRIFTRSDKCKVVIQ 121

HRAD9: 112 LHCKFGVRKTHNLSFQDCESLQAVFDPASCPHMLRAPARVLGEAVLPPSPALAEVTLGIG 171
             + G+ +THN+ FQ+ + LQ +FD   C + L     R+L +A++ F+ +  EVTL +
HRAD9B:122 FFYRHGIKRTHNICFQESQPLQVIFDKNVCTNTLMIQPRLLADAIVLFTSSQEEVTLAV- 180

HRAD9: 172 RGRRVILRSYHEEEADSTAKAMVTEMCLGEEDFQQLQAQFGVAITFCLKEFRGLLSFAES 231
             L+S +EE  D  + A+ +EM +G ++F   Q       ITFC KE +G+L+F+E+
HRAD9B:181 TPLNFCLKSSNEESMD-LSNAVHSEMFVGSDEFDFFQIGMDTEITFCFKELKGLLTFSEA 239

HRAD9: 232 ANLNLSIHFDAPGRPAIFTIKDSLLDGHFVLATLSDTDSHS---QDLGSPERHQPVPQLQ 288
             +  SI+FD PG+P   +I D L++ +F+LATL+D  S +   Q L   ++ +    ++
HRAD9B:240 THAPISIYFDFPGKPLALSIDDMLVEANFILATLADEQSRASSPQSLCLSQKRKRSDLIE 299

HRAD9: 289 AHSTPHPDDFANDDIDSYMIAMETTIGNEGSRVLPSISLSPGPQPPKSPGPHSEEFDEAE 348
             +  +   A + I S  A       E    + ++     P  +  G  SE  + +
HRAD9B:300 KKAGKNVTGQALECI-SKKAAPRRLYPKETLTNISALENCGSPAMKRVDGDVSEVSESSV 358

HRAD9: 349 PST  VPGTPPPKKFRSLFFGSILAPVR-SPQGPSPVLAEDSEGEG----------     391
             +T  VPG+   +KF  +FFG++ +        P   LA  S+ E
HRAD9B:359 SNTEEVPGSLCLRKFSCMFFGAVSSDQQEHFNHPFDSLARASDSEEDMNNGSFSIF     414



Mrad9: 1   MKCLITGGNVKVLGKAVHSLSRIGDELYLEPLKDGLSLRTVNSSRSAYACFLFAPLFFQQ 60
           -KC +TGG VKV GKAV +LSR+ DEL+L+P + GL+LR+VNS  S Y   LF+ +FFQ
Mrad9B:1   MLKCGMTGGQVKVFGKAVQTLSRVSDELWLDPSEKGLALRSVNSCHSTYGYVLFSSMFFQH 61

Mrad9: 61  YQ----AASPGQDL----LRCKILMKAFLSVFRSLAIVEKSVEKCCISLSGSHSHLVVQLH 113
           YQ    A     DL    L CK+ +K+ L +FR L  +E+SVEKC +         +V+Q
Mrad9B:62  YQWSPFATMSDTDLPLNLNCKLAIKSVLPIFRCLNYLERSVEKCTVVARADKCRVVIQFF 121

Mrad9: 114 CKYGVKKTHNLSFQDCFSLQAVFDPASCPHLLRTPARVLAEAVLSFPLALTFVTLGIGRG 173
            K-G+K+THN+ FQD + L+ +F+ + C ++L     R+L EA-         EVT  -  G
Mrad9B:122 GKHCIKRTHNVYFQDSQPLKIIFEKSLCANILMIKPRLLTEAIALLTSNQEEVTFSVTPG 181

Mrad9: 174 RRVILRSYQEEEADSTSKAMVTETSIGDEDFQQLHAPEGIAVTFCLKEFRGLLSFAESAN 233
             L+S   E  D TS ++ +E S G E+F           +TFC KE +G+L+F+E  +
Mrad9B:182 N-FCLKSLSGELLDLTS-SVYSEMSFGPEEFDFFQVGLDTEITFCFKELKGILTFSEVMH 239

Mrad9: 234 LPLTIHFDVPGRPVTFTIEDSLLDAHFVLATLLEQDSCSQGPCSPKPHQPVPQKQAHSTP 293
             PL I+FD PG+PV+ +ED LL+A+F+LATL++  S +  P      Q +P  QA  +
Mrad9B:240 APLAIYFDFPGKPVVLSVFDMLLEANFILATLVDYPSRTSSP-----  QLLPLSQARRSH 293

Mrad9: 294 HLDDFTSDDIDCYMIAMETTGGNEGSGAQPSTSLPPVSLASHDLAPTS----        341
           +      +D        E+      S A P    P  S  S   A T
Mrad9B:294 PIQSSAPFDKSRVSQTPEST-----SRAAPKRLFPKDSPDSSSAAETKRASAGQDDIFEV 348

Mrad9: 342  -------EEEAEPSTVPGTPPPKKFRSLFFGSILAPVHSPQG-PNPVLAEDSDGFG--- 388
                  EEE  PS +       +KF  +FFG++         G P   LA  SD E
Mrad9B:349 PESVVSDMEEERSPSIHL -----RKFSCMFFGAVSCEQQEYAGHPIDSLAVASDSKDVSG 398
```

Fig. 1. Amino acid sequence comparisons of the proteins encoded by *HRAD9*, *HRAD9B*, *Mrad9*, and *Mrad9B*. *Top*, HRAD9 *versus* HRAD9B; *bottom*, Mrad9 *versus* Mrad9B. A comparison of HRAD9 *versus* Mrad9 has already been published (2). Identical amino acids are cited between the complete sequence lists. A *plus* indicates amino acids that are not identical but have similar physiochemical properties.

(National Center for Biotechnology Information BLAST was used to compare sequences, and DNA Strider was used to determine ORFs). The accession number for the human genomic sequence is NT_009770, and according to the data bank, the gene maps to chromosome 12q24. A comparison with the corresponding cDNA sequence indicates that the gene is greater than 28 kb and contains 11 exons and 10 introns (Table 2). The accession numbers for three mouse genomic DNA sequence entries in the data bank are NW_0000236, AC093473, and AC113285. Each entry has a different portion of the genomic DNA. These *Mrad9B* sequences were located on mouse chromosome 5F. A comparison of the *Mrad9B* genomic and cDNA sequences revealed that this mouse gene had a structure similar to the human orthologue; that is, the gene was more than 28 kb long, with 11 exons and 10 introns (Table 2). In summary, *HRAD9B* and *Mrad9B* have identical intron-exon organization and encode proteins related at the amino acid level.

HRAD9B Protein Is Localized in the Nucleus and Can Coimmunoprecipitate with HRAD1, HRAD9, HHUS1, and HHUS1B Checkpoint Control Proteins. HRAD9 is a nucleoprotein (3, 4). The PSORT II computer program (40) predicts that HRAD9B contains a

Table 2 *Exon-intron structure of HRAD9B and Mrad9B*

Exon	Size (bp)	cDNA	5′ splice	Intron	Size (bp)	3′ splice
HRAD9B						
1	37	1–37	TGAAAGgtggag	1	1422	ccatagTATTTG
2	71	38–108	AAAGGTgtaagt	2	1740	ttctagCTTGCT
3	156	109–264	ATGAAGgtaaat	3	806	ttacagTCAATT
4	115	265–379	GACATGgtaggt	4	6085	tttaagGTATTA
5	100	380–479	ACCAAGgtaatg	5	2171	ttatagATTGCT
6	107	480–586	CAATGGgtaaag	6	3519	aaacagATTTGA
7	107	587–693	TTGAAGgtaaat	7	91	tttcagGGAATA
8	65	694–758	TGGGAAgtaggt	8	855	ttttagACCTCT
9	123	759–881	AAAAAGgtaaga	9	2260	cctcagGTCAGA
10	235	882–1116	AGAAAGgtaaaa	10	8113	ctccagTTTTCT
11	129	1117–1245				
Mrad9B						
1	37	1–37	TGAAAGgtggag	1	1524	ccatagTATTTG
2	71	38–108	AAAGGTgtaagt	2	833	ttccagCTTGCT
3	150	109–258	ATAAAGgtaaaa	3	187	ttgcagTCAGTT
4	115	259–373	AGCATGgtaggt	4	6962	tttaagGTATTA
5	100	374–473	ACCAAGgtaaag	5	4359	ttacagACTGCT
6	107	474–580	TGCTGGgtaagg	6	5215	aaccagATTTGA
7	107	581–687	CTGAAGgtaagc	7	83	ctgcagGGGATC
8	65	688–752	TGGAAAgtaggt	8	846	ttctagACCGGT
9	120	753–872	ACGAAGgtaatg	9	1598	gcccagGTCACA
10	229	873–1101	AGGAAGgtagga	10	5489	ttctagTTTTCC
11	111	1102–1212				

nuclear localization signal (*i.e.*, amino acids 289–292, KRKR) that is different from the one in HRAD9 (*i.e.*, amino acids 356–364, PPPKKFRSL; Ref. 41), in terms of both sequence and location. Therefore, we performed immunofluorescence experiments to determine whether HRAD9B also resides in the nuclear compartment of cells. We fused *HRAD9* and *HRAD9B* to a FLAG epitope, expressed these tagged genes in HeLa cells, and then visualized the proteins using fluorescence microscopy, probing for the tag. As indicated in Fig. 2, HRAD9B is found in the nucleus because the FITC stain colocalizes with the control DAPI stain. HRAD9 is also found primarily in the nucleus, as reported previously (3, 4).

Human cell cycle checkpoint control proteins HRAD9, HRAD1, and HHUS1 are all nucleoproteins and physically interact with each other (11). To determine whether HRAD9B shares this latter property, we determined whether the protein coimmunoprecipitates with the other checkpoint gene products as well as the HHUS1 paralogue, HHUS1B. As indicated in Fig. 3, all of the previously identified checkpoint genes were tagged with a FLAG epitope and individually coexpressed with HA-tagged HRAD9B in 293 cells. When HRAD9, HRAD1, HHUS1, or HHUS1B was immunoprecipitated with antibodies specific for FLAG, antibodies against HA consistently detected HA-HRAD9B via Western analysis. When the reverse was performed (that is, when antibodies against HA were used for the initial immunoprecipitation, and the presence of the other proteins was tested using antibodies against FLAG), HRAD9, HRAD1, and HHUS1 were detected repeatedly. However, HHUS1B was not always observed consistently through multiple repeat experiments. This result suggests that HRAD9B and HHUS1B physically interact, but perhaps weakly. The inconsistent result could also mean that the anti-HA antibody does not work well when HA-HRAD9B is bound to FLAG-HHUS1B.

***HRAD9B* and *Mrad9B* Are Expressed at High Levels Predominantly in the Testis.** Northern blot analysis was used to determine whether *HRAD9B* is expressed in a tissue-specific manner. As shown in Fig. 4, three strong bands are detected in testis, perhaps representing alternatively spliced RNA, but little or no corresponding message was found in 15 other human tissues. *Mrad9B* RNA was also pre-

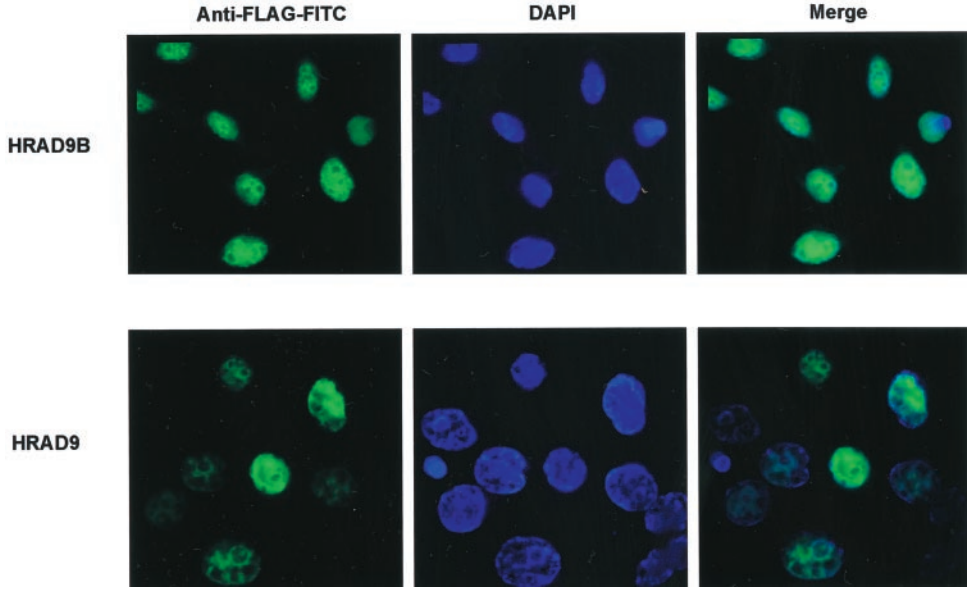

Fig. 2. Localization of HRAD9B and HRAD9 in the nucleus. HeLa cells were transfected with a plasmid encoding FLAG-tagged HRAD9B or HRAD9, and after 24 h, cells were stained with anti-FLAG antibodies to visualize these proteins or stained with DAPI to detect DNA in the nucleus. The untransfected control cells contained an undetectable FLAG signal (data not shown). As indicated, both HRAD9B and (as reported previously) HRAD9 localize in the nucleus.

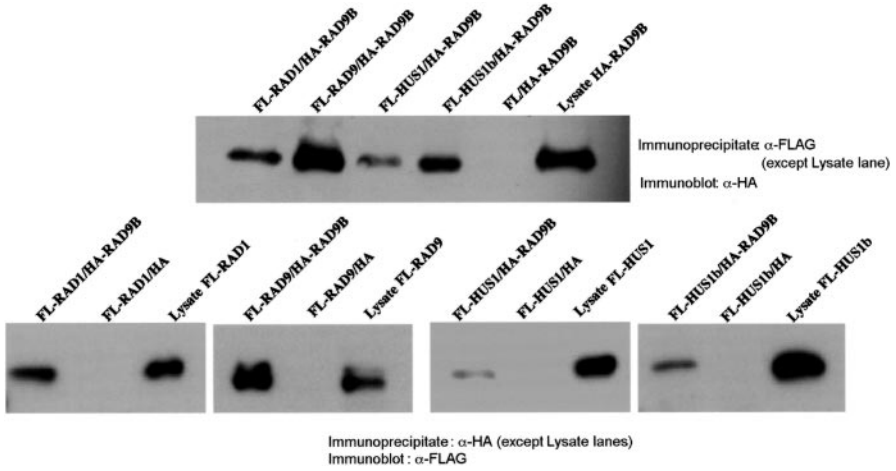

Fig. 3. Western analysis demonstrating that HRAD9B coimmunoprecipitates with the human checkpoint proteins HRAD1, HRAD9, HHUS1, and HHUS1B. Details are explained in the text. *Top* shows HRAD9B on the Western blot; *bottom* shows the other checkpoint proteins cited.

dominantly located in testis because two intense bands were observed in this tissue, but little or no message was detected in the eight other tissues examined. However, because the original *Mrad9B* sequence data bank entry was derived from a liver cDNA library, there is some, albeit very little, expression in at least this tissue as well as in testis. In contrast, as indicated in Fig. 4, *HRAD9* RNA is abundant in many different tissues, including testis. We reported previously (2) that *Mrad9* message is also detected in multiple mouse tissues.

***HRAD9B* RNA Levels Are Markedly Reduced in Testicular Tumors, Especially Seminomas.** *HRAD9B* is highly related to the *HRAD9* checkpoint control gene, whose multiple functions are characteristic of several tumor suppressors. Furthermore, it resides in chromosome 12q24 (contig/accession number NT_009770), close to a region previously linked to testicular cancers (*i.e.*, 12q22; 32). Therefore, *HRAD9B* abundance was examined by quantitative RT-PCR in normal and cancerous testicular tissue to establish a link between the levels of the message and cancer of this organ. As indicated in Fig. 5, a comparision of six normal adult testis samples (group I) and three genetically matched nonseminomas (group III, *2, *5, and *6), as well as three matched seminomas (group V, *1, *3, and *4) revealed that in every case the normal tissues contained significantly more *HRAD9B* RNA (relative to *GADPH* control). Four of six additional, unmatched nonseminomas also contained less *HRAD9B* RNA than the normal controls. However, all three additional unmatched seminomas had much less message than the six controls examined. These results indicate that *HRAD9B* RNA levels are significantly reduced in most nonseminoas (seven of nine tested), relative to normal tissue controls. However, the levels of *HRAD9B* RNA are consistently and most dramatically decreased in seminomas (six of six tested).

To test whether expression of *HRAD9B* is linked to meiosis, we examined corresponding message levels in fetal testis, a tissue that does not undergo this process but has the potential to do so. As indicated in Fig. 5*A* (group II), *HRAD9B* RNA is high in three fetal testis samples, relative to the *GADPH* RNA control. However, for two of the three independent samples, the levels overlap the low-end range of the adult normal testis tissues examined.

HRAD9B RNA level was also tested in one Leydig tumor sample. This non-germ cell tumor had message levels that bordered near the average detected in seminomas and nonseminomas.

Quantitative RT-PCR indicates a different RNA abundance pattern

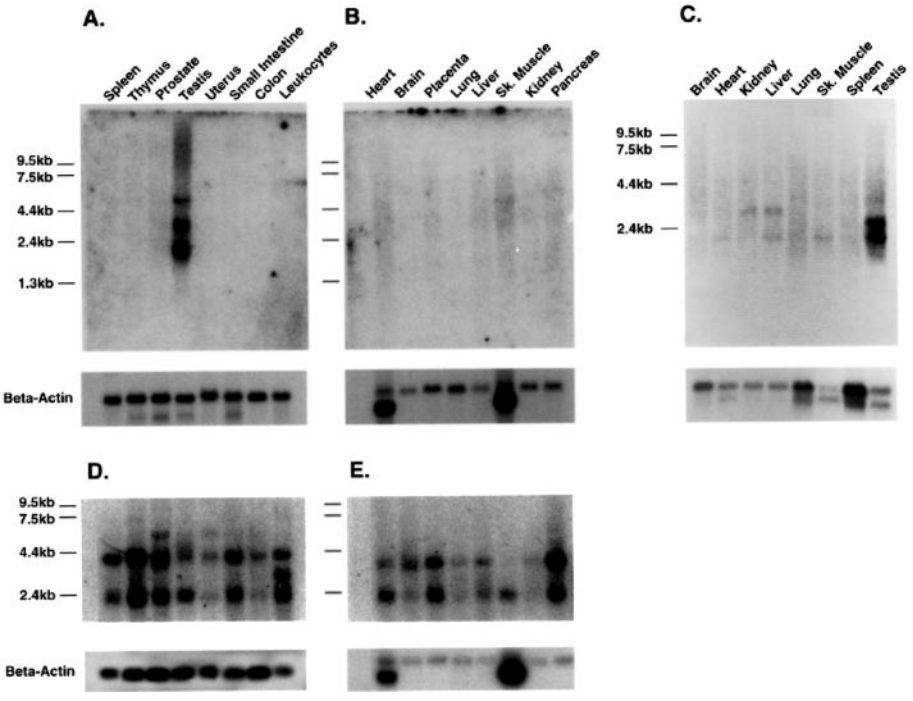

Fig. 4. Northern blot analysis indicates that *HRAD9B* and *Mrad9B* are expressed predominantly in testis, whereas *HRAD9* RNA is detected in many different tissues. Human (*A*, *B*, *D*, and *E*) and mouse (*C*) multitissue RNA blots were obtained from Clontech and Stratagene, respectively. Antisense *HRAD9B* and *Mrad9B* ^{32}P-labeled RNA probes and ^{32}P-labeled *HRAD9* cDNA fragments were made corresponding to the ORF of each gene and used to probe the blots (*HRAD9B*, blots *A*, *B*; *Mrad9B*, blot *C*; *HRAD9*, blots *D*, *E*). After washing and exposing X-ray film, blots were stripped, reprobed with ^{32}P-labeled β-actin cDNA, and again used to expose X-ray film (bottom of each blot). Three paralogue bands appear in the human *HRAD9B* blot, whereas two are present in mouse, likely indicative of alternatively spliced message. Alternatively spliced *HRAD9* RNA species are also detected. Northern blot results for *Mrad9* have been reported previously (2) and follow essentially the same pattern demonstrated by *HRAD9* RNA.

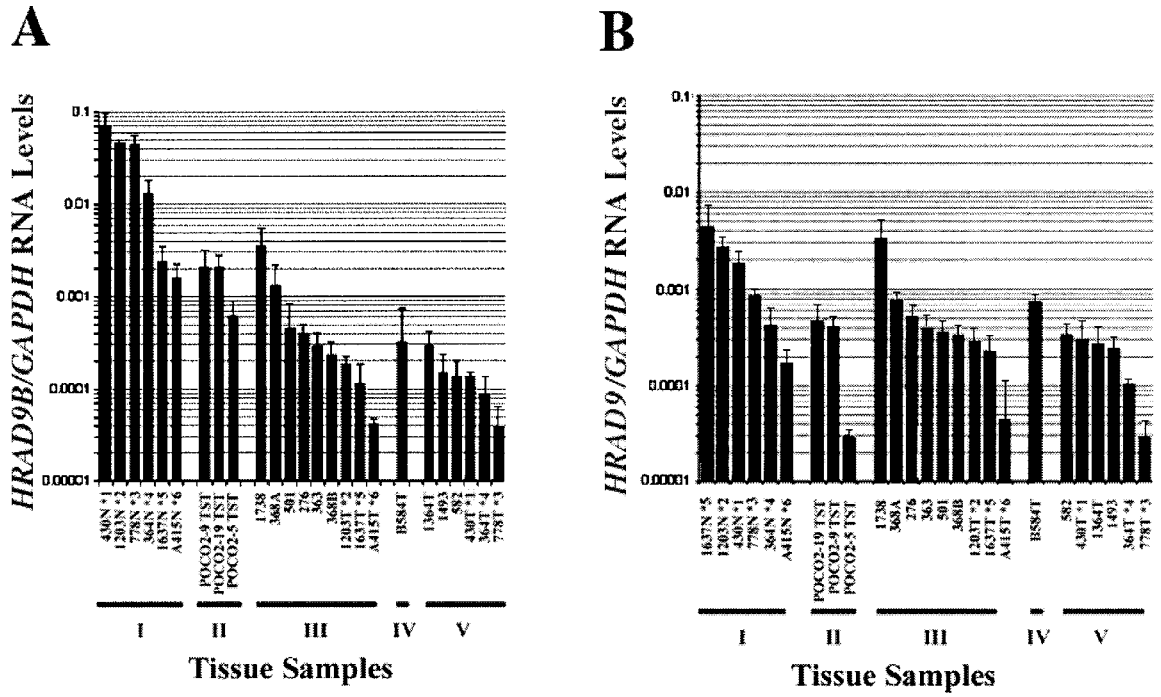

Fig. 5. Quantitative RT-PCR used to assess (*A*) *HRAD9B* and (*B*) *HRAD9* RNA levels in normal and cancerous testicular tissue. Table 1 lists and describes the tissue samples. Tissues are grouped as follows: I, normal adult testis; II, normal fetal testis; III, nonseminomatous germ cell tumor; IV, Leydig cell tumor; and V, seminoma. An *asterisk* followed by a *number* denotes normal/tumor tissue sample pairs that are genetically matched. Data are presented in descending order of *HRAD9B*/*GADPH* or *HRAD9*/*GADPH* levels for each group of samples. All *bars* represent the average of three independent trials ± SD.

for *HRAD9*. As shown in Fig. 5*B*, *HRAD9* message varies widely from sample to sample in each group of testicular tissue. This range of variation overlaps between groups, and therefore low or high abundance is not consistently associated with any one type of testicular tissue, albeit normal or tumor.

***HRAD17* RNA Levels in Normal and Cancerous Testicular Tissues.** A previous report (20) suggested that *HRAD17* RNA is also expressed at high levels in normal adult testis but is reduced in seminomas. However, this study used *in situ* hybridization on genetically unmatched tumor and normal histological tissue samples to make the assessment. Nevertheless, given this result and the known functional relationship between this gene and *HRAD9*, we examined levels of *HRAD17* RNA in the same set of samples used to determine *HRAD9B* abundance. As indicated in Fig. 6, quantitative RT-PCR showed that *HRAD17* RNA levels were high in normal adult testis (group I), on average higher than levels of *HRAD9B* (Fig. 5*A*, group I). However, unlike *HRAD9B* message levels, the abundance of *HRAD17* RNA was lower than that in the normal samples for all nine nonseminomas tested (group III). In addition, all six seminomas had low levels of *HRAD17* RNA, relative to adult control tissue, but the range was large (group V). As for the fetal testis samples (group II), two of three had levels of *HRAD17* RNA comparable with normal adult testis, but the third was very low. Again, the range of RNA abundance in fetal testis was greater than what was detected for *HRAD9B* in the same samples. In addition, the Leydig tumor had more *RAD17* RNA than the seminomas or nonseminomas. These results therefore indicate that *HRAD17* RNA levels are reduced in seminomas and nonseminomas, relative to normal adult tissue controls, but the magnitude of the normal/tumor differences varied, especially for the former tumor group, and the differences were generally not as dramatic as those for *RAD9B* message levels.

DISCUSSION

We have isolated human and mouse paralogues of previously identified mammalian orthologues of the fission yeast *S. pombe rad9* checkpoint control gene (1, 2, 42, 43). These paralogues are called *HRAD9B* and *Mrad9B*, respectively. All four of these mammalian genes have very similar structure, but homology comparisons and BLAST searches using the paralogues as query sequences indicate

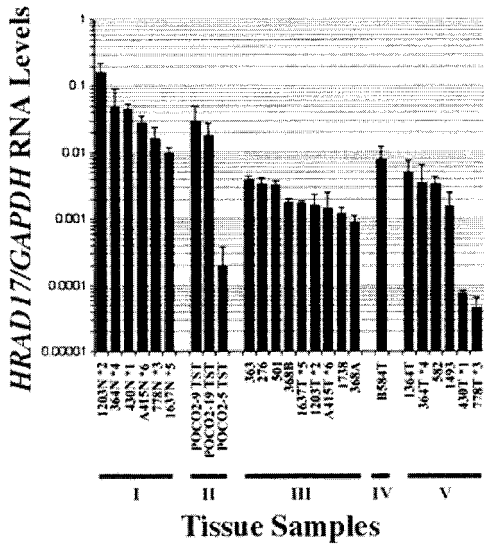

Fig. 6. Quantitative RT-PCR used to assess *HRAD17* RNA levels in normal and cancerous testicular tissue. Table 1 lists and describes the tissue samples. Tissues are grouped as follows: I, normal adult testis; II, normal fetal testis; III, nonseminomatous germ cell tumor; IV, Leydig cell tumor; and V, seminoma. An *asterisk* followed by a *number* denotes normal/tumor tissue sample pairs that are genetically matched. Data are presented in descending order of *HRAD17*/*GADPH* levels for each group of samples. All *bars* represent the average of three independent trials ± SD.

that *HRAD9B* and *Mrad9B* do not have equivalents in fission yeast or other nonmammalian organisms. These results suggest that *HRAD9B* and *Mrad9B* have evolved functions specific for higher eukaryotes. In mammals, paralogues of cell cycle (44) and recombination (45–47) genes have been described. These genes encode proteins that make up a family whose members have very similar structures and can often function coordinately as well. Recently, we isolated and characterized human and mouse paralogues of *HHUS1* (12), another checkpoint control gene, but its molecular function has not yet been defined in detail.

Studies with *HRAD9B* indicate that it has properties related to *HRAD9*. For example, both encoded proteins contain nuclear localization signals, albeit different ones, and do in fact reside in the nucleus. Furthermore, they can physically associate with the mammalian checkpoint control proteins HRAD9 (previous two-hybrid analysis indicated that two HRAD9 protein molecules can bind each other; Ref. 11), HRAD1, HHUS1, and HHUS1B. HRAD9B thus likely plays a role in cell cycle checkpoint control because it can associate with these other proteins involved in the process. Furthermore, HRAD9 and its *S. pombe* orthologue contain a BH3 domain through which they bind the antiapoptotic proteins Bcl-2 and Bcl-X_L and promote apoptosis (7, 8). Although HRAD9B has no obvious fission yeast equivalent, it does contain a BH3-like domain that differs from the region contained in HRAD9 by only a single amino acid. Therefore, it too is likely to be involved in mediating programmed cell death, but such a conclusion must await the generation of experimental support.

Although *HRAD9B* shares many characteristics with *HRAD9*, the two genes cannot solely possess completely redundant functions because they also have several different properties. For example, HRAD9 has a *S. pombe* ortholog, and HRAD9B has no obvious fission yeast equivalent. In addition, HRAD9 is hyperphosphorylated when cells are exposed to γ-rays or UV light (5, 48, 49), but HRAD9B is not modified in the same way in response to these DNA damaging agents.[4] Furthermore, *HRAD9* is expressed in many different tissues, whereas Northern blot analysis indicates that *HRAD9B* RNA appears confined predominantly to testis. Interestingly, several other checkpoint control genes are expressed at high levels in testis (2, 12–20). These results suggest that the proteins encoded by *HRAD9B* and at least some of these other checkpoint genes might function coordinately in the testis, perhaps as part of a meiotic checkpoint pathway (50).

In contrast to normal testicular tissue, we found that testicular tumors, and in particular seminomas, contain very little *HRAD9B* RNA. Similar studies with *HRAD9* did not reveal the same corresponding RNA abundance pattern. Interestingly, it has been known for some time that these kinds of tumors are highly radiosensitive (51), and patients who have not yet undergone radiotherapy demonstrate high levels of spontaneous chromosome instability (52). Another intriguing feature of human seminoma cells is that they cannot be cultured *in vitro* because attempts to do so result in extensive apoptosis (53). These characteristics suggest that the low levels of *HRAD9B*, which is structurally related to the radioresistance/apoptosis gene *HRAD9* and shares several biochemical properties with it as well, could be at least partly responsible for these attributes.

HRAD9B levels varied in samples over a 1789-fold range and were somewhat related to the meiotic potential of the cells. Normal adult testis tissue, which is able to undergo meiosis, contained the highest levels of *HRAD9B* RNA. Fetal testis had the next highest message levels on average and does not undergo robust meiosis but has the potential to do so after further development. In general, the testicular tumors (and in particular, the seminomas) contained less *HRAD9B* RNA than either the genetically matched or unmatched adult normal testicular tissues examined. Of the 16 tumor samples tested, only 2 had *HRAD9* RNA levels approaching those detected in normal adult testis. The seminomas, relative to the nonseminomas, which are a mixture of testicular tissue types, on average consistently contained the lowest levels of *HRAD9B*. Leydig cells, which are not derived directly from germ cells, showed *HRAD9B* levels between those determined for the seminomas and nonseminomas. Therefore, *HRAD9B* may be a marker for meiosis, as has been found for other genes (37, 38), in addition to perhaps having a more direct role in testicular cancer. *HRAD9B* does reside on chromosome 12q24 (contig/accession number NT_009770), very close to a region previously associated with alterations linked to seminomas (*i.e.*, 12q22; Ref. 32), suggesting a more direct role in the disease. Because HRAD9B associates with multiple cell cycle checkpoint control proteins and is structurally related to one, it likely also has a related function. Furthermore, these types of genes are believed to maintain genomic integrity, and their alteration is linked to carcinogenesis (26), again consistent with an important, direct role in testicular cancer.

A report by von Deimling *et al.* (20) showed that *HRAD17* RNA levels, demonstrated by *in situ* hybridization, were high in germinal epithelium of the seminiferous tubuli of six independent normal testis samples. However, four genetically unmatched seminomas had significantly reduced, diffuse, and weaker signals. We used quantitative RT-PCR to confirm this result. We found that, on average, the seminomas examined had lower levels of *HRAD17* RNA than adult testis, but the levels varied significantly between these tumor samples. Nonseminomas also demonstrated lower *HRAD17* levels than the normal controls, and levels varied less from sample to sample. There was some relationship between meiotic potential of the tissue and *HRAD17* RNA levels, although a stronger relationship was demonstrated for *HRAD9B*. Nevertheless, given the high levels of *HRAD17* and *HRAD9B* in normal testis, as well as the abundance of other checkpoint control gene RNAs in this tissue, it is possible that HRAD9B might work coordinately with HRAD17 as part of a checkpoint complex that monitors steps in meiosis for proper execution.

Data presented in this study describe human and mouse paralogues of the *HRAD9* and *Mrad9* checkpoint control genes, respectively. The link between testicular cancer, in particular seminomas, and the abundance of *HRAD9B* message suggests that an understanding of the biological role of the gene should help define the molecular basis for testicular germ cell cancer. The role of *HRAD9B* in relation to the function of the HRAD9-HRAD1-HHUS1 complex, as well as HRAD17, should also be important in this regard.

ACKNOWLEDGMENTS

We thank Dr. Charles R. Geard for providing imaging instruments and Dr. Adayabalam Balajee for technical guidance in relation to immunofluorescence studies. We are also grateful to Ayana Morales for technical assistance during many facets of this investigation.

REFERENCES

1. Lieberman, H. B., Hopkins, K. M., Nass, M., Demetrick, D., and Davey, S. A human homologue of the *Schizosaccharomyces pombe rad9*+ checkpoint control gene. Proc. Natl. Acad. Sci. USA, *93:* 13890–13895, 1996.
2. Hang, H., Rauth, S. J., Hopkins, K. M., Davey, S. K., and Lieberman, H. B. Molecular cloning and tissue-specific expression of *Mrad9*, a murine orthologue of the *Schizosaccharomyces pombe rad9*+ checkpoint control gene. J. Cell. Physiol., *177:* 232–240, 1998.
3. St. Onge, R. P., Udell, C. M., Casselman, R., and Davey, S. The human G_2 checkpoint control protein hRAD9 is a nuclear phosphoprotein that forms complexes with hRAD1 and hHUS1. Mol. Biol. Cell, *10:* 1985–1995, 1999.

[4] K. M. Hopkins and H. B. Lieberman, unpublished data.

4. Burtelow, M. A., Kaufmann, S. H., and Karnitz, L. M. Retention of the human Rad9 checkpoint complex in extraction-resistant nuclear complexes after DNA damage. J. Biol. Chem., *275:* 26343–26348, 2000.
5. Chen, M-J., Lin, Y-T., Lieberman, H. B., Chen, G., and Lee, E. Y-H. P. ATM-dependent phosphorylation of human Rad9 is required for ionizing radiation-induced checkpoint activation. J. Biol. Chem., *276:* 16580–16586, 2001.
6. Bessho, T., and Sancar, A. Human DNA damage checkpoint protein hRAD9 is a 3′ to 5′ exonuclease. J. Biol. Chem., *275:* 7451–7454, 2000.
7. Komatsu, K., Hopkins, K. M., Lieberman, H. B., and Wang, H-G. *Schizosaccharomyces pombe* Rad9 contains a BH3-like region and interacts with the anti-apoptotic protein Bcl-2. FEBS Lett., *481:* 122–126, 2000.
8. Komatsu, K., Miyashita, T., Hang, H., Hopkins, K. M., Zheng, W., Cuddeback, S., Yamada, M., Lieberman, H. B., and Wang, H-G. Human homologue of *S. pombe* Rad9 interacts with Bcl-2/Bcl-xL and promotes apoptosis. Nat. Cell Biol., *2:* 1–6, 2000.
9. Yoshida, K., Komatsu, K., Wang, H. G., and Kufe, D. c-Abl tyrosine kinase regulates the human Rad9 checkpoint protein in response to DNA damage. Mol. Cell. Biol., *22:* 3292–3300, 2002.
10. Yoshida, K., Wang, H. G., Miki, Y., and Kufe, D. Protein kinase Cδ is responsible for constitutive and DNA damage-induced phosphorylation of Rad9. EMBO J., *22:* 1431–1441, 2003.
11. Hang, H., and Lieberman, H. B. Physical interactions among human checkpoint control proteins HUS1p, RAD1p and RAD9p, and implications for the regulation of cell cycle progression. Genomics, *65:* 24–33, 2000.
12. Hang, H., Zhang, Y., Dunbrack, R. L., Jr., Wang, C., and Lieberman, H. B. Identification and characterization of a paralog of human cell cycle checkpoint gene, HUS1. Genomics, *79:* 487–492, 2002.
13. Keegan, K. S., Holtzman, D. A., Plug, A. W., Christenson, E. R., Brainerd, E. E., Flaggs, G., Bentley, N. J., Taylor, E. M., Meyn, M. S., Moss, S. B., Carr, A. M., Ashley, T., and Hoekstra, M. F. The Atr and Atm protein kinases associate with different sites along meiotically pairing chromosomes. Genes Dev., *10:* 2423–2437, 1996.
14. Pangilinan, F., Li, Q., Weaver, T., Lewis, B. C., Dang, C. V., and Spencer, F. Mammalian BUB1 protein kinases: map positions and *in vivo* expression. Genomics, *46:* 379–388, 1997.
15. Bluyssen, H. A., van Os, R. I., Naus, N. C., Jaspers, I., Hoeijmakers, J. H., and de Klein, A. A human and mouse homolog of the *Schizosaccharomyces pombe rad1+* cell cycle checkpoint control gene. Genomics, *54:* 331–337, 1998.
16. Freire, R., Murguia, J. R., Tarsounas, M., Lowndes, N. F., Moens, P. B., and Jackson, S. P. Human and mouse homologs of *Schizosaccharomyces pombe rad1+* and *Saccharomyces cerevisiae RAD17*: linkage to checkpoint control and mammalian meiosis. Genes Dev., *12:* 2560–2573, 1998.
17. Parker, A. E., Van de Weyer, I., Laus, M. C., Oostveen, I., Yon, J., Verhasselt, P., and Luyten, W. H. A human homologue of the *Schizosaccharomyces pombe rad1+* checkpoint gene encodes an exonuclease. J. Biol. Chem., *273:* 18332–18339, 1998.
18. Parker, A. E., Van de Weyer, I., Laus, M. C., Verhasselt, P., and Luyten, W. H. Identification of a human homologue of the *Schizosaccharomyces pombe rad17+* checkpoint gene. J. Biol. Chem., *273:* 18340–18346, 1998.
19. Bluyssen, H. A., Naus, N. C., van Os, R. I., Jaspers, I., Hoeijmakers, J. H., and de Klein, A. Human and mouse homologs of the *Schizosaccharomyces pombe rad17+* cell cycle checkpoint control gene. Genomics, *55:* 219–228, 1999.
20. von Deimling, F., Scharf, J. M., Liehr, T., Rothe, M., Kelter, A-R., Albers, P., Dietrich, W. F., Kunkel, L. M., Wernert, N., and Wirth, B. Human and mouse *RAD17* genes: identification, localization, genomic structure and histological expression pattern in normal testis and seminoma. Hum. Genet., *105:* 17–27, 1999.
21. Xu, Y., Ashley, T., Brainerd, E. E., Bronson, R. T., Meyn, M. S., and Baltimroe, D. Targeted disruption of *ATM* leads to growth retardation, chromosomal fragmentation during meiosis, immune defects, and thymic lymphoma. Genes Dev., *10:* 2411–2422, 1996.
22. Conner, F., Bertwistle, D., Mee, P. J., Ross, G. M., Swift, S., Grigorieva, E., Tybulewicz, V. L., and Ashworth, A. Tumorigenesis and a DNA repair defect in mice with a truncating *Brca2* mutation. Nat. Genet., *17:* 423–430, 1997.
23. Barlow, C., Lianage, M., Moens, P. B., Tarsounas, M., Nagashima, K., Brown, K., Rottinghaus, S., Jackson, S. P., Tagle, D., Ried, T., and Wynshaw-Boris, A. *Atm* deficiency in severe meiotic disruption as early as leptonema of prophase I. Development (Camb.), *125:* 4007–4017, 1998.
24. Pandita, T. K., Westphal, C. H., Anger, M., Sawant, S. G., Geard, C. R., Pandita, R. K., and Scherthan, H. *Atm* inactivation results in aberrant telomere clustering during meiotic prophase. Mol. Cell. Biol., *19:* 5096–5105, 1999.
25. Eaker, S., Cobb, J., Pyle, A., and Handel, M. A. Meiotic prophase abnormalities and metaphase cell death in MLH1-deficient mouse spermatocytes: insights into regulation of spermatogenic progress. Dev. Biol., *249:* 85–95, 2002.
26. Hartwell, L. H., and Kastan, M. B. Cell cycle control and cancer. Science (Wash. DC), *266:* 1821–1828, 1994.
27. Looijenga, L. H., de Munnik, H., and Oosterhuis, J. W. A molecular model for the development of germ cell cancer. Int. J. Cancer, *83:* 809–814, 1999.
28. Looijenga, L. H., and Oosterhuis, J. W. Pathogenesis of testicular germ cell tumours. Rev. Reprod., *4:* 90–100, 1999.
29. Jorgensen, N., Rajpert-De Meyts, E., Graem, N., Muller, J., Giwercman, A., and Skakkebaek, N. E. Expression of immunohistochemical markers for testicular carcinoma *in situ* by normal human fetal germ cells. Lab. Investig., *72:* 223–231, 1995.
30. Moller, H. Decreased testicular cancer risk in men born in wartime. J. Natl. Cancer Inst. (Bethesda), *81:* 1668–1669, 1989.
31. Skakkebaek, N. E. Possible carcinoma-*in-situ* of the testis. Lancet, *2:* 516–517, 1972.
32. Murty, V. V. S., Montgomery, K., Dutta, S., Bala, S., Renault, B., Bosl, G. J., Kucherlapati, R., and Chaganti, R. S. A 3-Mb high-resolution BAC/PAC contig of 12q22 encompassing the 830-kb consensus minimal deletion in male germ cell tumors. Genome Res., *9:* 662–671, 1999.
33. Qiao, D., Zeeman, A-M., Deng, W., Looijenga, L. H. J., and Lin, H. Molecular characterization of *hiwi*, a human member of the *piwi* gene family whose overexpression is correlated to seminomas. Oncogene, *21:* 3988–3999, 2002.
34. Mostofi, F. K., and Sesterhenn, I. A. Histological Typing of Testis Tumours, p. 132. Berlin: Springer, 1998.
35. Rajpert-De Meyts, E., Jorgensen, N., Muller, J., and Skakkebaek, N. E. Prolonged expression of the c-kit receptor in germ cells of intersex fetal testes. J. Pathol., *178:* 166–169, 1996.
36. Roelofs, H., Manes, T., Janszen, T., Millan, J. L., Oosterhuis, J. W., and Looijenga, L. H. Heterogeneity in alkaline phosphatase isozyme expression in human testicular germ cell tumours: an enzyme-/immunohistochemical and molecular analysis. J. Pathol., *189:* 236–244, 1999.
37. Dekker, I., Rozeboom, T., Delemarre, J., Dam, A., and Oosterhuis, J. W. Placental-like alkaline phosphatase and DNA flow cytometry in spermatocytic seminoma. Cancer (Phila.), *69:* 993–996, 1992.
38. Stoop, H., van Gurp, R., de Krijger, R., Geurts van Kessel, A., Koberle, B., Oosterhuis, W., and Looijenga, L. Reactivity of germ cell maturation stage-specific markers in spermatocytic seminoma: diagnostic and etiological implications. Lab. Investig., *81:* 919–928, 2001.
39. Jones, R. H., and Vasey, P. A. New directions in testicular cancer; molecular determinants of oncogenesis and treatment success. Eur. J. Cancer, *39:* 147–156, 2003.
40. Nakai, K., and Horton, P. PSORT: a program for detecting sorting signals in proteins and predicting their subcellular localization. Trends Biochem. Sci., *24:* 34–36, 1999.
41. Hirai, I., and Wang, H. G. A role of the C-terminal region of human Rad9 (hRad9) in nuclear transport of the hRad9 checkpoint complex. J. Biol. Chem., *277:* 25722–25727, 2002.
42. Murray, J. M., Carr, A. M., Lehmann, A. R., and Watts, F. Z. Cloning and characterization of the *rad9* DNA repair gene from *Schizosaccharomyces pombe*. Nucleic Acids Res., *19:* 3525–3531, 1991.
43. Lieberman, H. B., Hopkins, K. M., Laverty, M., and Chu, H. M. Molecular cloning and analysis of *Schizosaccharomyces pombe rad9*, a gene involved in DNA repair and mutagenesis. Mol. Gen. Genet., *232:* 367–376, 1992.
44. Nilsson, I., and Hoffmann, I. Cell cycle regulation by the Cdc25 phosphatase family. Prog. Cell Cycle Res., *4:* 107–114, 2000.
45. Takata, M., Sasaki, M. S., Tachiiri, S., Fukushima, T., Sonoda, E., Schild, D., Thompson, L. H., and Takeda, S. Chromosome instability and defective recombinational repair in knockout mutants of the five Rad51 paralogs. Mol. Cell. Biol., *21:* 2858–2866, 2001.
46. Wiese, C., Collins, D. W., Albala, J. S., Thompson, L. H., Kronenberg, A., and Schild, D. Interactions involving the Rad51 paralogs Rad51C and XRCC3 in human cells. Nucleic Acids Res., *30:* 1001–1008, 2002.
47. Liu, N., Schild, D., Thelen, M. P., and Thompson, L. H. Involvement of Rad51C in two distinct protein complexes of Rad51 paralogs in human cells. Nucleic Acids Res., *30:* 1009–1015, 2002.
48. Volkmer, E., and Karnitz, L. M. Human homologues of *Schizosaccharomyces pombe* rad1, hus1 and rad9 form a DNA damage-responsive protein complex. J. Biol. Chem., *274:* 567–570, 1999.
49. St. Onge, R. P., Besley, B. D., Park, M., Casselman, R., and Davey, S. DNA damage-dependent and -independent phosphorylation of the hRad9 checkpoint protein. J. Biol. Chem., *276:* 41898–41905, 2001.
50. Tarsounas, M., and Moens, P. B. Checkpoint and DNA-repair proteins are associated with the cores of mammalian meiotic chromosomes. Curr. Top. Dev. Biol., *51:* 109–134, 2001.
51. Stutzman, R. E., and McLeod, D. G. Radiation therapy: a primary treatment modality for seminoma. Urol. Clin. N. Am., *7:* 757–764, 1980.
52. Schmidberger. H., Virsik-Koepp, P., Rave-Frank, M., Reinosch, K. R., Pradier, O., Munzel, U., and Hess, C. F. Reciprocal translocations in patients with testicular seminoma before and after radiotherapy. Int. J. Radiat. Oncol. Biol. Phys., *50:* 857–864, 2001.
53. Olie, R. A., Boersma, A. W., Dekker, M. C., Nooter, K., Looijenga, L. H., and Oosterhuis, J. W. Apoptosis of human seminoma cells upon disruption of their microenvironment. Br. J. Cancer, *73:* 1031–1036, 1996.